Chapter 3

The Zimm model

3.1 Hydrodynamic interactions in a Gaussian chain

In the previous chapter we have focused on the Rouse chain, which gives a good description of the dynamics of unentangled *concentrated* polymer solutions and melts. We will now add hydrodynamic interactions between the beads of a Gaussian chain. This so-called Zimm chain, gives a good description of the dynamics of unentangled *dilute* polymer solutions.

The equations describing hydrodynamic interactions between beads, up to lowest order in the bead separations, are given by

$$\mathbf{v}_i = -\sum_{j=0}^{N} \bar{\boldsymbol{\mu}}_{ij} \cdot \mathbf{F}_j \tag{3.1}$$

$$\bar{\boldsymbol{\mu}}_{ii} = \frac{1}{6\pi\eta_s a}\bar{\mathbf{I}}, \qquad \bar{\boldsymbol{\mu}}_{ij} = \frac{1}{8\pi\eta_s R_{ij}}\left(\bar{\mathbf{I}} + \hat{\mathbf{R}}_{ij}\hat{\mathbf{R}}_{ij}\right). \tag{3.2}$$

Here $\mathbf{v}_i$ is the velocity of bead i, $\mathbf{F}_j$ the force exerted by the fluid on bead j, η_s the solvent viscosity, a the radius of a bead, and $\hat{\mathbf{R}}_{ij} = \mathbf{R}_{ij}/R_{ij}$, where $\mathbf{R}_{ij} = \mathbf{R}_i - \mathbf{R}_j$ is the vector from the position of bead j to the position of bead i. A derivation can be found in Appendix A of this chapter.

In Eq. (3.1), the mobility tensors $\bar{\boldsymbol{\mu}}$ relate the bead velocities to the hydrodynamic forces acting on the beads. Of course there are also conservative forces $-\boldsymbol{\nabla}_k\Phi$ acting on the beads because they are connected by springs. On the Smoluchowski time scale, we assume that the conservative forces make the beads move with constant velocities $\mathbf{v}_k$. This amounts to saying that the forces $-\boldsymbol{\nabla}_k\Phi$ are exactly balanced by the hydrodynamic forces acting on the beads k. In Appendix B we describe the Smoluchowski equation for the beads in a Zimm chain. The

Langevin equations corresponding to this Smoluchowski equation are

$$\frac{d\mathbf{R}_j}{dt} = -\sum_k \bar{\boldsymbol{\mu}}_{jk} \cdot \nabla_k \Phi + k_B T \sum_k \nabla_k \cdot \bar{\boldsymbol{\mu}}_{jk} + \mathbf{f}_j \tag{3.3}$$

$$\langle \mathbf{f}_j(t) \rangle = \mathbf{0} \tag{3.4}$$

$$\langle \mathbf{f}_j(t)\mathbf{f}_k(t') \rangle = 2k_B T \bar{\boldsymbol{\mu}}_{jk}\delta(t-t'). \tag{3.5}$$

The reader can easily check that these reduce to the equations of motion of the Rouse chain when hydrodynamic interactions are neglected.

The particular form of the mobility tensor Eq. (3.2) (the Oseen tensor) has the fortunate property

$$\sum_k \nabla_k \cdot \bar{\boldsymbol{\mu}}_{jk} = \mathbf{0}, \tag{3.6}$$

which greatly simplifies Eq. (3.3).

3.2 Normal modes and Zimm relaxation times

If we introduce the mobility tensors Eq. (3.2) into the Langevin equations (3.3) - (3.5), we are left with a completely intractable set of equations. One way out of this is by noting that in equilibrium, on average, the mobility tensor will be proportional to the unit tensor. A simple calculation yields

$$\begin{aligned}
\langle \bar{\boldsymbol{\mu}}_{jk} \rangle_{\text{eq}} &= \frac{1}{8\pi\eta_s} \left\langle \frac{1}{R_{jk}} \right\rangle_{\text{eq}} \left(\bar{\mathbf{I}} + \langle \hat{\mathbf{R}}_{jk}\hat{\mathbf{R}}_{jk} \rangle_{\text{eq}} \right) \\
&= \frac{1}{6\pi\eta_s} \left\langle \frac{1}{R_{jk}} \right\rangle_{\text{eq}} \bar{\mathbf{I}} \\
&= \frac{1}{6\pi\eta_s b} \left(\frac{6}{\pi|j-k|} \right)^{\frac{1}{2}} \bar{\mathbf{I}}
\end{aligned} \tag{3.7}$$

The next step is to write down the equations of motion of the Rouse modes, using Eqs. (2.35) and (2.37):

$$\frac{d\mathbf{X}_p}{dt} = -\sum_{q=1}^N \mu_{pq}\frac{3k_B T}{b^2}4\sin^2\left(\frac{q\pi}{2(N+1)}\right)\mathbf{X}_q + \mathbf{F}_p \tag{3.8}$$

$$\langle \mathbf{F}_p(t) \rangle = \mathbf{0} \tag{3.9}$$

$$\langle \mathbf{F}_p(t)\mathbf{F}_q(t') \rangle = k_B T \frac{\mu_{pq}}{N+1}\bar{\mathbf{I}}\delta(t-t'), \tag{3.10}$$

where

$$\mu_{pq} = \frac{2}{N+1} \sum_{j=0}^{N} \sum_{k=0}^{N} \frac{1}{6\pi\eta_s b} \left(\frac{6}{\pi|j-k|} \right)^{\frac{1}{2}} \cos\left[\frac{p\pi}{N+1}(j+\frac{1}{2}) \right] \cos\left[\frac{q\pi}{N+1}(k+\frac{1}{2}) \right]. \tag{3.11}$$

Eq. (3.8) is still not tractable. It turns out however (see Appendix C for a proof) that for large N approximately

$$\mu_{pq} = \left(\frac{N+1}{3\pi^3 p} \right)^{\frac{1}{2}} \frac{1}{\eta_s b} \delta_{pq}. \tag{3.12}$$

Introducing this result in Eq. (3.8), we see that the Rouse modes, just like with the Rouse chain, constitute a set of decoupled coordinates of the Zimm chain:

$$\frac{d\mathbf{X}_p}{dt} = -\frac{1}{\tau_p}\mathbf{X}_p + \mathbf{F}_p \tag{3.13}$$

$$\langle \mathbf{F}_p(t) \rangle = \mathbf{0} \tag{3.14}$$

$$\langle \mathbf{F}_p(t)\mathbf{F}_q(t') \rangle = k_B T \frac{\mu_{pp}}{N+1} \bar{\mathbf{I}} \delta_{pq} \delta(t-t'), \tag{3.15}$$

where the first term on the right hand side of Eq. (3.13) equals zero when $p = 0$, and otherwise, for $p \ll N$,

$$\tau_p \approx \frac{3\pi\eta_s b^3}{k_B T} \left(\frac{N+1}{3\pi p} \right)^{\frac{3}{2}}. \tag{3.16}$$

Eqs. (3.13) - (3.15) lead to the same exponential decay of the normal mode auto-correlations as in the case of the Rouse chain,

$$\langle \mathbf{X}_p(t) \cdot \mathbf{X}_p(0) \rangle = \langle X_p^2 \rangle \exp(-t/\tau_p), \tag{3.17}$$

but with a different distribution of relaxation times τ_p. Notably, the relaxation time of the slowest mode, $p = 1$, scales as $N^{\frac{3}{2}}$ instead of N^2. The amplitudes of the normal modes, however, are the same as in the case of the Rouse chain,

$$\langle X_p^2 \rangle \approx \frac{(N+1)b^2}{2\pi^2} \frac{1}{p^2}. \tag{3.18}$$

This is because both the Rouse and Zimm chains are based on the same static model (the Gaussian chain), and only differ in the details of the friction, i.e. they only differ in their kinetics.

3.3 Dynamic properties of a Zimm chain

The diffusion coefficient of (the centre-of-mass of) a Zimm chain can easily be calculated from Eqs. (3.13) - (3.15). The result is

$$
\begin{aligned}
D_G &= \frac{k_BT}{2}\frac{\mu_{00}}{N+1} = \frac{k_BT}{6\pi\eta_s b}\sqrt{\frac{6}{\pi}}\frac{1}{(N+1)^2}\sum_{j=0}^{N}\sum_{k=0}^{N}\frac{1}{|j-k|^{\frac{1}{2}}}\\
&\approx \frac{k_BT}{6\pi\eta_s b}\sqrt{\frac{6}{\pi}}\frac{1}{N^2}\int_0^N\mathrm{d}j\int_0^N\mathrm{d}k\,\frac{1}{|j-k|^{\frac{1}{2}}} = \frac{8}{3}\frac{k_BT}{6\pi\eta_s b}\sqrt{\frac{6}{\pi N}}.
\end{aligned}\tag{3.19}
$$

The diffusion coefficient now scales with $N^{-1/2}$, in agreement with experiments on dilute polymer solutions.

   The similarities between the Zimm chain and the Rouse chain enable us to quickly calculate various other dynamic properties. For example, the time correlation function of the end-to-end vector is given by Eq. (2.53), but now with the relaxation times τ_p given by Eq. (3.16). Similarly, the segmental motion can be found from Eq. (2.55), and the shear relaxation modulus (excluding the solvent contribution) from Eq. (2.79). Hence, for dilute polymer solutions, the Zimm model predicts an intrinsic viscosity given by

$$
[\eta] = \frac{\eta-\eta_s}{\rho\eta_s} = \frac{N_{\mathrm{Av}}k_BT}{M\eta_s}\sum_{p=1}^{N}\frac{\tau_p}{2} = \frac{N_{\mathrm{Av}}}{M}12\pi\left[\frac{(N+1)b^2}{12\pi}\right]^{\frac{3}{2}}\sum_{p=1}^{N}\frac{1}{p^{\frac{3}{2}}},\tag{3.20}
$$

where ρ is the polymer concentration and M is the mol mass of the polymer. The intrinsic viscosity scales with $N^{1/2}$ (remember that $M\propto N$), again in agreement with experiments on dilute polymer solutions.

Problems

3-1. Proof the last step in Eq. (3.7) [Hint: the Zimm chain is a Gaussian chain].

3-2. Check Eq. (3.18) explicitly from Eqs. (3.12) and (3.16) and by noting that

$$
0 = \frac{\mathrm{d}}{\mathrm{d}t}\left\langle \mathbf{X}_p(t)\cdot\mathbf{X}_p(t)\right\rangle = -\frac{2}{\tau_p}\left\langle \mathbf{X}_p(t)\cdot\mathbf{X}_p(t)\right\rangle + 2\left\langle \mathbf{F}_p(t)\cdot\mathbf{X}_p(t)\right\rangle
$$

in equilibrium, where the last term is equal to

$$
2\int_0^t\mathrm{d}\tau\,e^{-(t-\tau)/\tau_p}\left\langle \mathbf{F}_p(t)\cdot\mathbf{F}_p(\tau)\right\rangle = \int_{-\infty}^{\infty}\mathrm{d}\tau\,e^{-|t-\tau|/\tau_p}\left\langle \mathbf{F}_p(t)\cdot\mathbf{F}_p(\tau)\right\rangle.
$$

3-3. Proof the first step in Eq. (3.19). [Hint: remember that the centre-of-mass is given by $\mathbf{X}_0$].

Appendix A: Derivation of hydrodynamic interactions in a suspension of spheres

In Appendix A of chapter 2 we calculated the flow field in the solvent around a *single* slowly moving sphere. When more than one sphere is present in the system, this flow field will be felt by the other spheres. As a result these spheres experience a force which is said to result from hydrodynamic interactions with the original sphere.

We will assume that at each time the fluid flow field can be treated as a steady state flow field. This is true for very slow flows, where changes in positions and velocities of the spheres take place over much larger time scales than the time it takes for the fluid flow field to react to such changes. The hydrodynamic problem then is to find a flow field satisfying the stationary Stokes equations,

$$\eta_s \nabla^2 \mathbf{v} = \nabla P \tag{A.1}$$
$$\nabla \cdot \mathbf{v} = 0, \tag{A.2}$$

together with the boundary conditions

$$\mathbf{v}(\mathbf{R}_i + \mathbf{a}) = \mathbf{v}_i \qquad \forall i, \tag{A.3}$$

where $\mathbf{R}_i$ is the position vector and $\mathbf{v}_i$ is the velocity vector of the i'th sphere, and $\mathbf{a}$ is any vector of length a. If the spheres are very far apart we may approximately consider any one of them to be alone in the fluid. The flow field is then just the sum of all flow fields emanating from the different spheres

$$\mathbf{v}(\mathbf{r}) = \sum_i \mathbf{v}_i^{(0)}(\mathbf{r} - \mathbf{R}_i), \tag{A.4}$$

where, according to Eq. (A.13),

$$
\begin{aligned}
\mathbf{v}_i^{(0)}(\mathbf{r} - \mathbf{R}_i) = {} & \mathbf{v}_i \frac{3a}{4\,|\mathbf{r} - \mathbf{R}_i|} \left[1 + \frac{a^2}{3(\mathbf{r} - \mathbf{R}_i)^2} \right] \\
& + (\mathbf{r} - \mathbf{R}_i)((\mathbf{r} - \mathbf{R}_i) \cdot \mathbf{v}_i) \frac{3a}{4\,|\mathbf{r} - \mathbf{R}_i|^3} \left[1 - \frac{a^2}{(\mathbf{r} - \mathbf{R}_i)^2} \right].
\end{aligned}
\tag{A.5}
$$

We shall now calculate the correction to this flow field, which is of lowest order in the sphere separation.

We shall first discuss the situation for only two spheres in the fluid. In the neighbourhood of sphere one the velocity field may be written as

$$\mathbf{v}(\mathbf{r}) = \mathbf{v}_1^{(0)}(\mathbf{r} - \mathbf{R}_1) + \frac{3a}{4\,|\mathbf{r} - \mathbf{R}_2|} \left[\mathbf{v}_2 + \frac{(\mathbf{r} - \mathbf{R}_2)}{|\mathbf{r} - \mathbf{R}_2|} \frac{(\mathbf{r} - \mathbf{R}_2)}{|\mathbf{r} - \mathbf{R}_2|} \cdot \mathbf{v}_2 \right], \tag{A.6}$$

where we have approximated $\mathbf{v}_2^{(0)}(\mathbf{r} - \mathbf{R}_2)$ to terms of order $a/|\mathbf{r} - \mathbf{R}_2|$. On the surface of sphere one we approximate this further by

$$\mathbf{v}(\mathbf{R}_1 + \mathbf{a}) = \mathbf{v}_1^{(0)}(\mathbf{a}) + \frac{3a}{4R_{21}} \left(\mathbf{v}_2 + \hat{\mathbf{R}}_{21}\hat{\mathbf{R}}_{21} \cdot \mathbf{v}_2\right), \tag{A.7}$$

where $\hat{\mathbf{R}}_{21} = (\mathbf{R}_2 - \mathbf{R}_1)/|\mathbf{R}_2 - \mathbf{R}_1|$. Because $\mathbf{v}_1^{(0)}(\mathbf{a}) = \mathbf{v}_1$, we notice that this result is not consistent with the boundary condition $\mathbf{v}(\mathbf{R}_1 + \mathbf{a}) = \mathbf{v}_1$. In order to satisfy this boundary condition we subtract from our results so far, a solution of Eqs. (A.1) and (A.2) which goes to zero at infinity, and which on the surface of sphere one corrects for the second term in Eq. (A.7). The flow field in the neighbourhood of sphere one then reads

$$\begin{aligned}
\mathbf{v}(\mathbf{r}) &= \mathbf{v}_1^{\text{corr}} \frac{3a}{4|\mathbf{r} - \mathbf{R}_1|} \left[1 + \frac{a^2}{3(\mathbf{r} - \mathbf{R}_1)^2}\right] \\
&\quad + (\mathbf{r} - \mathbf{R}_1)((\mathbf{r} - \mathbf{R}_1) \cdot \mathbf{v}_1^{\text{corr}}) \frac{3a}{4|\mathbf{r} - \mathbf{R}_1|^3} \left[1 - \frac{a^2}{(\mathbf{r} - \mathbf{R}_1)^2}\right] \\
&\quad + \frac{3a}{4R_{21}} \left(\mathbf{v}_2 + \hat{\mathbf{R}}_{21}\hat{\mathbf{R}}_{21} \cdot \mathbf{v}_2\right)
\end{aligned} \tag{A.8}$$

$$\mathbf{v}_1^{\text{corr}} = \mathbf{v}_1 - \frac{3a}{4R_{21}} \left(\mathbf{v}_2 + \hat{\mathbf{R}}_{21}\hat{\mathbf{R}}_{21} \cdot \mathbf{v}_2\right). \tag{A.9}$$

The flow field in the neighbourhood of sphere two is treated similarly.

We notice that the correction that we have applied to the flow field in order to satisfy the boundary conditions at the surface of sphere one is of order a/R_{21}. Its strength in the neighbourhood of sphere two is then of order $(a/R_{21})^2$, and need therefore not be taken into account when the flow field is adapted to the boundary conditions at sphere two.

The flow field around sphere one is now given by Eqs. (A.8) and (A.9). The last term in Eq. (A.8) does not contribute to the stress tensor (the gradient of a constant field is zero). The force exerted by the fluid on sphere one then equals $-6\pi\eta_s a \mathbf{v}_1^{\text{corr}}$. A similar result holds for sphere two. In full we have

$$\mathbf{F}_1 = -6\pi\eta_s a \mathbf{v}_1 + 6\pi\eta_s a \frac{3a}{4R_{21}} \left(\bar{\mathbf{I}} + \hat{\mathbf{R}}_{21}\hat{\mathbf{R}}_{21}\right) \cdot \mathbf{v}_2 \tag{A.10}$$

$$\mathbf{F}_2 = -6\pi\eta_s a \mathbf{v}_2 + 6\pi\eta_s a \frac{3a}{4R_{21}} \left(\bar{\mathbf{I}} + \hat{\mathbf{R}}_{21}\hat{\mathbf{R}}_{21}\right) \cdot \mathbf{v}_1, \tag{A.11}$$

where $\bar{\mathbf{I}}$ is the three-dimensional unit tensor. Inverting these equations, retaining only terms up to order a/R_{21}, we get

$$\mathbf{v}_1 = -\frac{1}{6\pi\eta_s a}\mathbf{F}_1 - \frac{1}{8\pi\eta_s R_{21}} \left(\bar{\mathbf{I}} + \hat{\mathbf{R}}_{21}\hat{\mathbf{R}}_{21}\right) \cdot \mathbf{F}_2 \tag{A.12}$$

$$\mathbf{v}_2 = -\frac{1}{6\pi\eta_s a}\mathbf{F}_2 - \frac{1}{8\pi\eta_s R_{21}} \left(\bar{\mathbf{I}} + \hat{\mathbf{R}}_{21}\hat{\mathbf{R}}_{21}\right) \cdot \mathbf{F}_1 \tag{A.13}$$

When more than two spheres are present in the fluid, corrections resulting from n-body interactions ($n \geq 3$) are of order $(a/R_{ij})^2$ or higher and need not be taken into account. The above treatment therefore generalizes to

$$\mathbf{F}_i = -\sum_{j=0}^{N} \bar{\boldsymbol{\zeta}}_{ij} \cdot \mathbf{v}_j \tag{A.14}$$

$$\mathbf{v}_i = -\sum_{j=0}^{N} \bar{\boldsymbol{\mu}}_{ij} \cdot \mathbf{F}_j, \tag{A.15}$$

where

$$\bar{\boldsymbol{\zeta}}_{ii} = 6\pi\eta_s a\bar{\mathbf{I}}, \qquad \bar{\boldsymbol{\zeta}}_{ij} = -6\pi\eta_s a\frac{3a}{4R_{ij}}\left(\bar{\mathbf{I}}+\hat{\mathbf{R}}_{ij}\hat{\mathbf{R}}_{ij}\right) \tag{A.16}$$

$$\bar{\boldsymbol{\mu}}_{ii} = \frac{1}{6\pi\eta_s a}\bar{\mathbf{I}}, \qquad \bar{\boldsymbol{\mu}}_{ij} = \frac{1}{8\pi\eta_s R_{ij}}\left(\bar{\mathbf{I}}+\hat{\mathbf{R}}_{ij}\hat{\mathbf{R}}_{ij}\right). \tag{A.17}$$

$\bar{\boldsymbol{\mu}}_{ij}$ is generally called the mobility tensor. The specific form Eq. (A.17) is known as the Oseen tensor.

Appendix B: Smoluchowski equation for the Zimm chain

For sake of completeness, we will describe the Smoluchowski equation for the beads in a Zimm chain. The equation is similar to, but a generalized version of, the Smoluchowski equation for a single bead treated in Appendix B of chapter 2.

Let $\Psi(\mathbf{R}_0,\ldots,\mathbf{R}_N;t)$ be the probability density of finding beads $0,\ldots,N$ near $\mathbf{R}_0,\ldots,\mathbf{R}_N$ at time t. The equation of particle conservation can be written as

$$\frac{\partial\Psi}{\partial t} = -\sum_{j=0}^{N} \boldsymbol{\nabla}_j \cdot \mathbf{J}_j, \tag{B.1}$$

where $\mathbf{J}_j$ is the flux of beads j. This flux may be written as

$$\mathbf{J}_j = -\sum_k \bar{\mathbf{D}}_{jk} \cdot \boldsymbol{\nabla}_k\Psi - \sum_k \bar{\boldsymbol{\mu}}_{jk} \cdot (\boldsymbol{\nabla}_k\Phi)\,\Psi. \tag{B.2}$$

The first term in Eq. (B.2) is the flux due to the random displacements of all beads, which results in a flux along the negative gradient of the probability density. The second term results from the forces $-\boldsymbol{\nabla}_k\Phi$ felt by all the beads. On the Smoluchowski time scale, these forces make the beads move with constant velocities $\mathbf{v}_k$, i.e., the forces $-\boldsymbol{\nabla}_k\Phi$ are exactly balanced by the hydrodynamic forces acting on

the beads k. Introducing these forces into Eq. (A.15), we find the systematic part of the velocity of bead j:

$$\mathbf{v}_j = -\sum_k \bar{\boldsymbol{\mu}}_{jk} \cdot (\boldsymbol{\nabla}_k \Phi). \tag{B.3}$$

Multiplying this by Ψ, we obtain the systematic part of the flux of particle j.

At equilibrium, each flux $\mathbf{J}_j$ must be zero and the distribution must be equal to the Boltzmann distribution $\Psi_{\text{eq}} = C \exp[-\beta\Phi]$. Using this in Eq. (B.2) it follows that

$$\bar{\mathbf{D}}_{jk} = k_B T \bar{\boldsymbol{\mu}}_{jk}, \tag{B.4}$$

which is a generalization of the Einstein equation.

Combining Eqs. (B.1), (B.2), and (B.4) we find the Smoluchowski equation for the beads in a Zimm chain:

$$\frac{\partial \Psi}{\partial t} = \sum_j \sum_k \boldsymbol{\nabla}_j \cdot \bar{\boldsymbol{\mu}}_{jk} \cdot (\boldsymbol{\nabla}_k \Phi + k_B T \boldsymbol{\nabla}_k \ln \Psi) \Psi. \tag{B.5}$$

Using techniques similar to those used in Appendix B of chapter 2, it can be shown that the Langevin Eqs. (3.3) - (3.5) are equivalent to the above Smoluchowski equation.

Appendix C: Derivation of Eq. (3.12)

In order to derive Eq. (3.12) we write

$$
\begin{aligned}
\mu_{pq} &= \frac{2}{N+1} \frac{1}{6\pi\eta_s b} \sqrt{\frac{6}{\pi}} \sum_{j=0}^{N} \cos\left[\frac{p\pi}{N+1}\left(j+\frac{1}{2}\right)\right] \times \\
&\quad \sum_{k=j-N}^{j} \cos\left[\frac{q\pi}{N+1}\left(j-k+\frac{1}{2}\right)\right] \frac{1}{\sqrt{|k|}} \\
&= \frac{2}{N+1} \frac{1}{6\pi\eta_s b} \sqrt{\frac{6}{\pi}} \sum_{j=0}^{N} \cos\left[\frac{p\pi}{N+1}\left(j+\frac{1}{2}\right)\right] \cos\left[\frac{q\pi}{N+1}\left(j+\frac{1}{2}\right)\right] \times \\
&\quad \sum_{k=j-N}^{j} \cos\left(\frac{q\pi k}{N+1}\right) \frac{1}{\sqrt{|k|}} \\
&\quad + \frac{2}{N+1} \frac{1}{6\pi\eta_s b} \sqrt{\frac{6}{\pi}} \sum_{j=0}^{N} \cos\left[\frac{p\pi}{N+1}\left(j+\frac{1}{2}\right)\right] \sin\left[\frac{q\pi}{N+1}\left(j+\frac{1}{2}\right)\right] \times \\
&\quad \sum_{k=j-N}^{j} \sin\left(\frac{q\pi k}{N+1}\right) \frac{1}{\sqrt{|k|}}. \tag{C.1}
\end{aligned}
$$

Figure 3.1: Contour for integration in the complex plane, Eq. (C.4). Part I is a line along the real axis from $x = 0$ to $x = R$, part II is a semicircle $z = Re^{i\phi}$, where $\phi \in \,]0, \pi/4]$, and part III is the diagonal line $z = (1 + i)x$, where $x \in \,]0, R/\sqrt{2}]$.
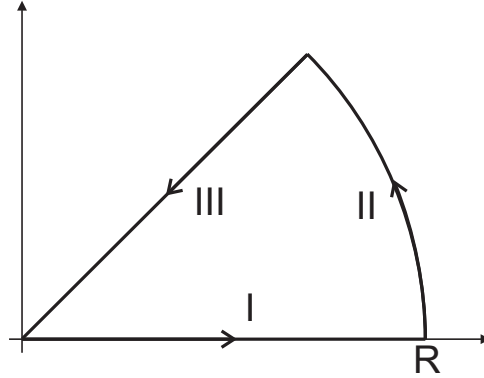
We now approximate

$$\sum_{k=j-N}^{j} \cos\left(\frac{q\pi k}{N+1}\right) \frac{1}{\sqrt{|k|}} \approx \int_{-\infty}^{\infty} dk \, \cos\left(\frac{q\pi k}{N+1}\right) \frac{1}{\sqrt{|k|}}$$

$$= 4 \int_0^{\infty} dx \, \cos\left(\frac{q\pi x^2}{N+1}\right) = \sqrt{\frac{2(N+1)}{q}} \quad \text{(C.2)}$$

$$\sum_{k=j-N}^{j} \sin\left(\frac{q\pi k}{N+1}\right) \frac{1}{\sqrt{|k|}} \approx \int_{-\infty}^{\infty} dk \, \sin\left(\frac{q\pi k}{N+1}\right) \frac{1}{\sqrt{|k|}} = 0. \quad \text{(C.3)}$$

The result of Eq. (C.3) is obvious because the integrand is an odd function of k. The last equality in Eq. (C.2) can be found by considering the complex function $f(z) = \exp(iaz^2)$ for any positive real number a on the contour given in Fig. 3.1. Because $f(z)$ is analytic (without singularities) on all points on and within the contour, the contour integral of $f(z)$ must be zero. We now write

$$\begin{aligned} 0 &= \oint dz \, e^{iaz^2} = \int_{(I)} dz \, e^{iaz^2} + \int_{(II)} dz \, e^{iaz^2} + \int_{(III)} dz \, e^{iaz^2} \\ &= \int_0^R dx \, e^{iax^2} + \int_0^{\pi/4} d\phi \, iRe^{i\phi + iaR^2 e^{2i\phi}} + \int_{R/\sqrt{2}}^0 dx \, (1+i)e^{ia[(1+i)x]^2} \\ &= \int_0^R dx \, e^{iax^2} + \int_0^{\pi/4} d\phi \, iRe^{i\phi + iaR^2 \cos 2\phi - aR^2 \sin 2\phi} - (1+i) \int_0^{R/\sqrt{2}} dx \, e^{-2ax^2} \end{aligned}$$

$$\text{(C.4)}$$

Taking the limit $R \to \infty$ the second term vanishes, after which the real part of the equation yields

$$\int_0^{\infty} dx \, \cos(ax^2) = \int_0^{\infty} dx \, e^{-2ax^2} = \sqrt{\frac{\pi}{8a}}. \quad \text{(C.5)}$$

Introducing Eqs. (C.2) and (C.3) into Eq. (C.1) one finds Eq. (3.12). As a technical detail we note that in principle diagonal terms in Eq. (3.11) should have

been treated separately, which is clear from Eq. (A.17). Since the contribution of all other terms is proportional to $N^{1/2}$, however, we omit the diagonal terms.

Chapter 4

The tube model

4.1 Entanglements in dense polymer systems

In the Rouse model we have assumed that interactions between different chains can be treated through some effective friction coefficient. As we have seen, this model applies well to melts of short polymer chains. In the Zimm model we have assumed that interactions between different chains can be ignored altogether, and only *intra*chain hydrodynamic interactions need to be taken into account. This model applies well to dilute polymer systems.

We will now treat the case of long polymer chains at high concentration or in the melt state. Studies of the mechanical properties of such systems reveal a nontrivial molecular weight dependence of the viscosity and rubber-like elastic behavior on time scales which increase with chain length. The observed behavior is rather universal, independent of temperature or molecular species (as long as the polymer is linear and flexible), which indicates that the phenomena are governed by the general nature of polymers. This general nature is, of course, the fact that the chains are intertwined and can not penetrate through each other: they are "entangled" (see Fig. 4.1). These topological interactions seriously affect the dynamical properties since they impose constraints on the motion of the polymers.

Figure 4.1: A simplified picture of polymer chains at high density. The chains are intertwined and cannot penetrate through each other.
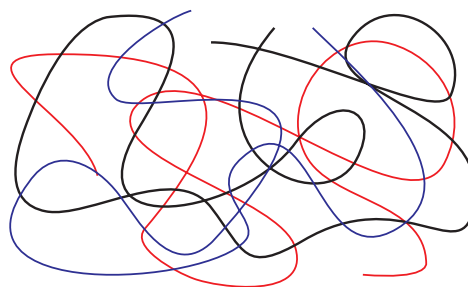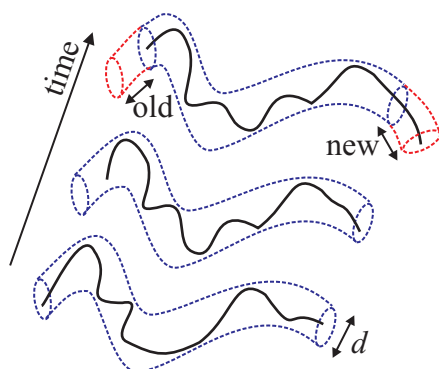
Figure 4.2: Representation of a polymer in a tube. The tube is due to surrounding chains, i.e. entanglements, so that the polymer can only reptate along the tube.

4.2   The tube model

In the tube model, introduced by De Gennes and further refined by Doi and Edwards, the complicated topological interactions are simplified to an effective tube surrounding each polymer chain. In order to move over large distances, the chain has to leave the tube by means of longitudinal motions. This concept of a tube clearly has only a statistical (mean field) meaning. The tube can change by two mechanisms. First by means of the motion of the central chain itself, by which the chain leaves parts of its original tube, and generates new parts. Secondly, the tube will fluctuate because of motions of the chains which build up the tube. It is generally believed that tube fluctuations of the second kind are unimportant for extremely long chains. For the case of medium long chains, subsequent corrections can be made to account for fluctuating tubes.

Let us now look at the mechanisms which allow the polymer chain to move along the tube axis, which is also called the primitive chain.

The chain of interest fluctuates around the primitive chain. By some fluctuation it may store some excess mass in part of the chain, see Fig. 4.2. This mass may diffuse along the primitive chain and finally leave the tube. The chain thus creates a new piece of tube and at the same time destroys part of the tube at the other side. This kind of motion is called *reptation*. Whether the tube picture is indeed correct for concentrated polymer solutions or melts still remains a matter for debate, but many experimental and simulation results suggest that reptation is the dominant mechanism for the dynamics of a chain in the highly entangled state.

It is clear from the above picture that the reptative motion will determine the long time motion of the chain. The main concept of the model is the primitive chain. The details of the polymer itself are to a high extent irrelevant. We may therefore choose a convenient polymer as we wish. Our polymer will again be a Gaussian chain. Its motion will be governed by the Langevin equations at the Smoluchowski time scale. Our basic chain therefore is a Rouse chain.

4.3 Definition of the model

The tube model consists of two parts. First we have the basic chain, and secondly we have the tube and its motion. So:

- Basic chain
  Rouse chain with parameters N, b and ζ.

- Primitive chain

  1. The primitive chain has contour length L, which is assumed to be constant. The position along the primitive chain will be indicated by the continuous variable $s \in [0, L]$. The configurations of the primitive chain are assumed to be Gaussian; by this we mean that

  $$\left\langle \left(\mathbf{R}(s) - \mathbf{R}(s') \right)^2 \right\rangle = d \left| s - s' \right|, \tag{4.1}$$

  where d is a new parameter having the dimensions of length. It is the step length of the primitive chain, or the tube diameter.

  2. The primitive chain can move back and forth only along itself with diffusion coefficient

  $$D_G = \frac{k_B T}{(N+1)\zeta}, \tag{4.2}$$

  i.e., with the Rouse diffusion coefficient, because the motion of the primitive chain corresponds to the overall translation of the Rouse chain along the tube.

The Gaussian character of the distribution of primitive chain conformations is consistent with the reptation picture, in which the chain continuously creates new pieces of tube, which may be chosen in random directions with step length d.

Apparently we have introduced two new parameters, the contour length L and the step length d. Only one of them is independent, however, because they are related by the end-to-end distance of the chain, $\langle R^2 \rangle = N b^2 = dL$, where the first equality stems from the fact that we are dealing with a Rouse chain, and the second equality follows from Eq. (4.1).

4.4 Segmental motion

We shall now demonstrate that according to our model the mean quadratic displacement of a typical monomer behaves like in Fig. (4.3). This behaviour has
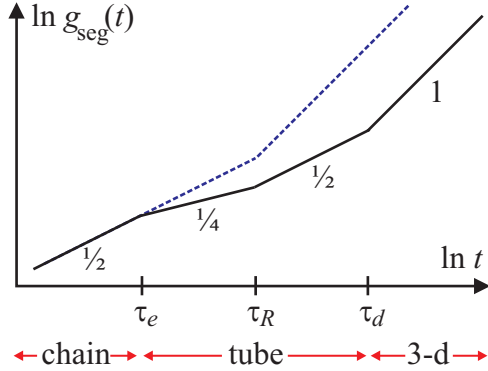
Figure 4.3: Logarithmic plot of the segmental mean square displacement, in case of the reptation model (solid line) and the Rouse model (dashed line).

been qualitatively verified by computer simulations. Of course the final regime should be simple diffusive motion. The important prediction is the dependence of the diffusion constant on N.

In Fig. (4.3), τ_R is the Rouse time which is equal to τ_1 in Eq. (2.46). The meaning of τ_e and τ_d will become clear in the remaining part of this section. We shall now treat the different regimes in Fig. (4.3) one after another.

i) $t \leq \tau_e$

At short times a Rouse bead does not know about any tube constraints. According to Eq. (2.57) then

$$g_{\text{seg}}(t) = \left(\frac{12kTb^2}{\pi\zeta} \right)^{\frac{1}{2}} t^{\frac{1}{2}}. \tag{4.3}$$

Once the segment has moved a distance equal to the tube diameter d, it will feel the constraints of the tube, and a new regime will set in. The time at which this happens is given by the entanglement time

$$\tau_e = \frac{\pi\zeta}{12k_BTb^2}d^4. \tag{4.4}$$

Notice that this is independent of N.

ii) $\tau_e < t \leq \tau_R$

On the time and distance scale we are looking now, the bead performs random motions, still constrained by the fact that the monomer is a part of a chain because $t \leq \tau_R$. Orthogonally to the primitive chain these motions do not lead to any displacement, because of the constraints implied by the tube. Only along the primitive chain the bead may diffuse free of any other constraint than the one

implied by the fact that it belongs to a chain. The diffusion therefore is given by the 1-dimensional analog of Eq. (2.57) or Eq. (4.3),

$$\langle (s_n(t) - s_n(0))^2 \rangle = \frac{1}{3} \left(\frac{12kTb^2}{\pi\zeta} \right)^{\frac{1}{2}} t^{\frac{1}{2}}, \tag{4.5}$$

where $s_n(t)$ is the position of bead n along the primitive chain at time t. It is assumed here that for times $t \leq \tau_R$ the chain as a whole does not move, i.e. that the primitive chain does not change. Using Eq. (4.1) then

$$g_{\text{seg}}(t) = d \left(\frac{4k_B T b^2}{3\pi\zeta} \right)^{\frac{1}{4}} t^{\frac{1}{4}}, \tag{4.6}$$

where we have assumed $\langle |s_n(t) - s_n(0)| \rangle \approx \langle (s_n(t) - s_n(0))^2 \rangle^{\frac{1}{2}}$.

iii) $\tau_R < t \leq \tau_d$

The bead still moves along the tube diameter. Now however $t > \tau_R$, which means that we should use the 1-dimensional analog of Eq. (2.56):

$$\langle (s_n(t) - s_n(0))^2 \rangle = 2D_G t. \tag{4.7}$$

Again assuming that the tube does not change appreciably during time t, we get

$$g_{\text{seg}}(t) = d \left[\frac{2k_B T}{(N+1)\zeta} \right]^{\frac{1}{2}} t^{\frac{1}{2}}. \tag{4.8}$$

From our treatment it is clear that τ_d is the time it takes for the chain to create a tube which is uncorrelated to the old one, or the time it takes for the chain to get disentangled from its old surroundings. We will calculate the disentanglement time τ_d in the next paragraph.

iv) $\tau_d < t$

This is the regime in which reptation dominates. On this time and space scale we may attribute to every bead a definite value of s. We then want to calculate

$$\varphi(s,t) = \langle (\mathbf{R}(s,t) - \mathbf{R}(s,0))^2 \rangle, \tag{4.9}$$

where $\mathbf{R}(s,t)$ is the position of bead s at time t. In order to calculate $\varphi(s,t)$ it is useful to introduce

$$\varphi(s,s';t) = \langle (\mathbf{R}(s,t) - \mathbf{R}(s',0))^2 \rangle, \tag{4.10}$$
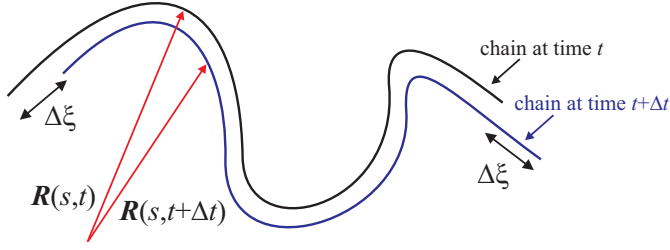
Figure 4.4: Motion of the primitive chain along its contour.

i.e. the mean square distance between bead s at time t and bead s' at time zero. According to Fig. (4.4), for all s, except $s = 0$ and $s = L$, we have

$$\varphi(s, s'; t + \Delta t) = \langle \varphi(s + \Delta \xi, s'; t) \rangle, \tag{4.11}$$

where $\Delta \xi$ according to the definition of the primitive chain in section 4.3 is a stochastic variable. The average on the right hand side has to be taken over the distribution of $\Delta \xi$. Expanding the right hand side of Eq. (4.11) we get

$$\begin{aligned}
\langle \varphi(s + \Delta \xi, s'; t) \rangle &\approx \varphi(s, s'; t) + \langle \Delta \xi \rangle \frac{\partial}{\partial s} \varphi(s, s'; t) + \frac{1}{2} \langle (\Delta \xi)^2 \rangle \frac{\partial^2}{\partial s^2} \varphi(s, s'; t) \\
&= \varphi(s, s'; t) + D_G \Delta t \frac{\partial^2}{\partial s^2} \varphi(s, s'; t).
\end{aligned} \tag{4.12}$$

Introducing this into Eq. (4.11) and taking the limit for Δt going to zero, we get

$$\frac{\partial}{\partial t} \varphi(s, s'; t) = D_G \frac{\partial^2}{\partial s^2} \varphi(s, s'; t). \tag{4.13}$$

In order to complete our description of reptation we have to find the boundary conditions going with this diffusion equation. We will demonstrate that these are given by

$$\begin{aligned}
\varphi(s, s'; t)|_{t=0} &= d|s - s'| \tag{4.14} \\
\frac{\partial}{\partial s} \varphi(s, s'; t)|_{s=L} &= d \tag{4.15} \\
\frac{\partial}{\partial s} \varphi(s, s'; t)|_{s=0} &= -d. \tag{4.16}
\end{aligned}$$

The first of these is obvious. The second follows from

$$\frac{\partial}{\partial s}\phi(s,s';t)|_{s=L} = 2\left\langle \frac{\partial \mathbf{R}(s,t)}{\partial s}|_{s=L}\cdot(\mathbf{R}(L,t)-\mathbf{R}(s',0))\right\rangle$$

$$= 2\left\langle \frac{\partial \mathbf{R}(s,t)}{\partial s}|_{s=L}\cdot(\mathbf{R}(L,t)-\mathbf{R}(s',t))\right\rangle$$

$$+2\left\langle \frac{\partial \mathbf{R}(s,t)}{\partial s}|_{s=L}\cdot(\mathbf{R}(s',t)-\mathbf{R}(s',0))\right\rangle$$

$$= 2\left\langle \frac{\partial \mathbf{R}(s,t)}{\partial s}|_{s=L}\cdot(\mathbf{R}(L,t)-\mathbf{R}(s',t))\right\rangle$$

$$= \frac{\partial}{\partial s}\left\langle (\mathbf{R}(s,t)-\mathbf{R}(s',t))^2\right\rangle|_{s=L} = \frac{\partial}{\partial s}d|s-s'||_{s=L}. \quad (4.17)$$

Condition Eq. (4.16) follows from a similar reasoning.

We now solve Eqs. (4.13)–(4.16), obtaining

$$\phi(s,s';t) = |s-s'|d+2D_G\frac{d}{L}t$$

$$+4\frac{Ld}{\pi^2}\sum_{p=1}^{\infty}\frac{1}{p^2}(1-e^{-tp^2/\tau_d})\cos\left(\frac{p\pi s}{L}\right)\cos\left(\frac{p\pi s'}{L}\right), \quad (4.18)$$

where

$$\tau_d = \frac{L^2}{\pi^2 D_G} = \frac{1}{\pi^2}\frac{b^4}{d^2}\frac{\zeta}{k_B T}N^3. \quad (4.19)$$

We shall not derive this here. The reader may check that Eq. (4.18) indeed is the solution to Eq. (4.13) satisfying (4.14)-(4.16).

Notice that τ_d becomes much larger than τ_R for large N, see Eq. (2.46). If the number of steps in the primitive chain is defined by $Z = Nb^2/d^2 = L/d$, then the ratio between τ_d and τ_R is $3Z$.

Taking the limit $s \to s'$ in Eq. (4.18) we get

$$\left\langle (\mathbf{R}(s,t)-\mathbf{R}(s,0))^2\right\rangle = 2D_G\frac{d}{L}t+4\frac{Ld}{\pi^2}\sum_{p=1}^{\infty}\cos^2\left(\frac{p\pi s}{L}\right)(1-e^{-tp^2/\tau_d})\frac{1}{p^2}. \quad (4.20)$$

For $t > \tau_d$ we get diffusive behaviour with diffusion constant

$$D = \frac{1}{3}D_G\frac{d}{L} = \frac{1}{3}\frac{d^2}{b^2}\frac{k_B T}{\zeta}\frac{1}{N^2}. \quad (4.21)$$

Notice that this is proportional to N^{-2}, whereas the diffusion coefficient of the Rouse model was proportional to N^{-1}. The reptation result, N^{-2}, is confirmed by experiments which measured the diffusion coefficients of polymer melts as a function of their molecular weight.
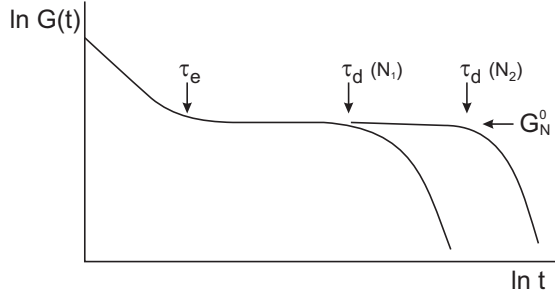
Figure 4.5: Schematic logaritmic plot of the time behaviour of the shear relaxation modulus $G(t)$ as measured in a concentated polymer solution or melt; $N_1 < N_2$.

4.5 Viscoelastic behaviour

Experimentally the shear relaxation modulus $G(t)$ of a concentrated polymer solution or melt turns out to be like in Fig. 4.5. We distinguish two regimes.

i) $t < \tau_e$

At short times the chain behaves like a 3-dimensional Rouse chain. Using Eq. (2.79) we find

$$
\begin{aligned}
G(t) &= \frac{ck_BT}{N+1} \sum_{p=1}^{N} \exp(-2t/\tau_p) \\
&\approx \frac{ck_BT}{N+1} \int_0^\infty \mathrm{d}p \, \exp(-2p^2t/\tau_R) \\
&= \frac{ck_BT}{N+1} \sqrt{\frac{\pi\tau_R}{8t}},
\end{aligned}
\tag{4.22}
$$

which decays as $t^{-\frac{1}{2}}$. At $t = \tau_e$ this possibility to relax ends. The only way for the chain to relax any further is by breaking out of the tube.

ii) $t > \tau_e$

The stress that remains in the system is caused by the fact that the chains are trapped in twisted tubes. By means of reptation the chain can break out of its tube. The newly generated tube contains no stress. So, it is plausible to assume that the stress at any time t is proportional to the fraction of the original tube that is still part of the tube at time t. We'll call this fraction $\Psi(t)$. So,

$$
G(t) = G_N^0 \Psi(t). \tag{4.23}
$$

On the reptation time scale, τ_e is practically zero, so we can set $\Psi(\tau_e) = \Psi(0) = 1$. To make a smooth transition from the Rouse regime to the reptation regime, we

match Eq. (4.22) with Eq. (4.23) at $t = \tau_e$, yielding

$$G_N^0 = \frac{ck_BT}{N+1}\sqrt{\frac{\pi\tau_R}{8\tau_e}} = \frac{ck_BT}{\sqrt{2\pi}}\frac{b^2}{d^2}. \tag{4.24}$$

Notice that the plateau value G_N^0 is independent of the chain length N. The numerical prefactor of $1/\sqrt{2\pi}$ in Eq. (4.24) is not rigorous because in reptation theory the time τ_e, at which the Rouse-like modulus is supposed to be instantaneously replaced by the reptation-like modulus, is not defined in a rigorous manner. A more precise calculation based on stress relaxation after a large step strain gives a numerical prefactor of 4/5, i.e.

$$G_N^0 = \frac{4}{5}\frac{ck_BTb^2}{d^2} = \frac{4}{5}\frac{ck_BT}{N_e}. \tag{4.25}$$

In the last equation we have defined the entanglement length N_e. In most experiments the entanglement length (or more precisely the entanglement molecular weight) is estimated from the value of the plateau modulus, using Eq. (4.25).

We will now calculate $\Psi(t)$. Take a look at

$$\left\langle \mathbf{u}\left(s',t\right)\cdot\mathbf{u}\left(s,0\right)\right\rangle \equiv \left\langle \frac{\partial\mathbf{R}\left(s',t\right)}{\partial s'}\cdot\frac{\partial\mathbf{R}\left(s,0\right)}{\partial s}\right\rangle. \tag{4.26}$$

The vector $\mathbf{u}\left(s',t\right)$ is the tangent to the primitive chain, at segment s' at time t. Because the primitive chain has been parametrized with the contour length, we have from Eq. (4.1) $\langle\mathbf{u}\cdot\mathbf{u}\rangle = \langle\Delta\mathbf{R}\cdot\Delta\mathbf{R}\rangle/\left(\Delta s\right)^2 = d/\Delta s$; the non-existence of the limit of $\triangle s$ going to zero is a peculiarity of a Gaussian process. Using Eqs. (4.10) and (4.18) we calculate

$$\begin{aligned}\left\langle \mathbf{u}\left(s',t\right)\cdot\mathbf{u}\left(s,0\right)\right\rangle &= -\frac{1}{2}\frac{\partial^2}{\partial s\partial s'}\varphi\left(s',s;t\right)\\ &= d\delta\left(s-s'\right)-\frac{2d}{L}\sum_{p=1}^{\infty}\left(1-e^{-tp^2/\tau_d}\right)\sin\left(\frac{p\pi s}{L}\right)\sin\left(\frac{p\pi s'}{L}\right)\\ &= \frac{2d}{L}\sum_{p=1}^{\infty}e^{-tp^2/\tau_d}\sin\left(\frac{p\pi s}{L}\right)\sin\left(\frac{p\pi s'}{L}\right),\end{aligned} \tag{4.27}$$

where we have used

$$\frac{2}{L}\sum_{p=1}^{\infty}\sin\left(\frac{p\pi s}{L}\right)\sin\left(\frac{p\pi s'}{L}\right) = \delta\left(s-s'\right). \tag{4.28}$$

Using this last equation, we also find

$$\left\langle \mathbf{u}\left(s',0\right)\cdot\mathbf{u}\left(s,0\right)\right\rangle = d\delta\left(s-s'\right). \tag{4.29}$$
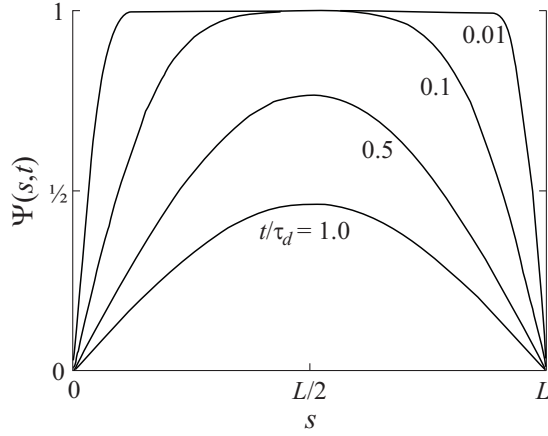
Figure 4.6: Development of $\Psi(s,t)$ in time.

This equation states that there is no correlation between the tangents to the primitive chain at a segment s, and at another segment s'. If we consider $\langle \mathbf{u}(s',t) \cdot \mathbf{u}(s,0) \rangle$ as a function of s', at time t, we see that the original delta function has broadened and lowered. However, the tangent $\mathbf{u}(s',t)$ can only be correlated to $\mathbf{u}(s,0)$ by means of diffusion of segment s', during the time interval $[0,t]$, to the place where s was at time $t = 0$, and still lies in the original tube. So, $\frac{1}{d}\langle \mathbf{u}(s',t) \cdot \mathbf{u}(s,0) \rangle$ is the probability density that, at time t, segment s' lies within the original tube at the place where s was initially. Integrating over s' gives us the probability $\Psi(s,t)$ that at time t *any* segment lies within the original tube at the place where segment s was initially. In other words, the chance that the original tube segment s is still up-to-date, is

$$
\begin{aligned}
\Psi(s,t) &= \frac{1}{d}\int_0^L \mathrm{d}s' \ \langle \mathbf{u}(s',t) \cdot \mathbf{u}(s,0) \rangle \\
&= \frac{4}{\pi}\sideset{}{'}\sum_{p=1}^{\infty} \frac{1}{p} \sin\left(\frac{p\pi s}{L}\right) \mathrm{e}^{-tp^2/\tau_d},
\end{aligned} \tag{4.30}
$$

where the prime at the summation sign indicates that only terms with odd p should occur in the sum. We have plotted this in Fig. 4.6. The fraction of the original tube that is still intact at time t, is therefore given by

$$
\begin{aligned}
\Psi(t) &= \frac{1}{L}\int_0^L \mathrm{d}s \ \Psi(s,t) \\
&= \frac{8}{\pi^2}\sideset{}{'}\sum_{p=1}^{\infty} \frac{1}{p^2} \mathrm{e}^{-tp^2/\tau_d}.
\end{aligned} \tag{4.31}
$$

This formula shows why τ_d is the time needed by the chain to reptate out if its tube; for $t > \tau_d$, $\Psi(t)$ is falling to zero quickly.

In conclusion we have found results that are in good agreement with Fig. 4.5. We see an initial drop proportional to $t^{-1/2}$; after that a plateau value G_N^0 independent of N; and finally a maximum relaxation time τ_d proportional to N^3.

Finally, we are able to calculate the viscosity of a concentrated polymer solution or melt of reptating chains. Using Eq. 2.70 we find

$$
\begin{aligned}
\eta &= \int_0^\infty d\tau\, G(\tau) = G_N^0 \frac{8}{\pi^2} \sum_{p=1}^{\infty}{}' \frac{1}{p^2} \int_0^\infty d\tau\, e^{-\tau p^2/\tau_d} \\
&= G_N^0 \frac{8}{\pi^2} \tau_d \sum_{p=1}^{\infty}{}' \frac{1}{p^4} = \frac{\pi^2}{12} G_N^0 \tau_d.
\end{aligned}
\tag{4.32}
$$

Since G_N^0 is independent of N, the viscosity, like τ_d, is proportional to N^3. This is close to the experimentally observed scaling $\eta \propto N^{3.4}$. The small discrepancy may be removed by introducing other relaxation modes in the tube model, which is beyond the scope of these lecture notes.

Problems

4-1. In Eq. (4.22) we have shown that, at short times, the shear relaxation modulus $G(t)$ decays as $t^{-\frac{1}{2}}$. We know, however, that $G(t)$ must be finite at $t = 0$. Explain how the stress relaxes at extremely short times. Draw this in Fig. 4.5.

4-2. In the tube model we have assumed that the primitive chain has a fixed contour length L. In reality, the contour length of a primitive chain can fluctuate in time. Calculations of a Rouse chain constrained in a straight tube of length L show that the average contour length fluctuation is given by

$$
\Delta \bar{L} = \langle \Delta L^2 \rangle^{\frac{1}{2}} \approx \left(\frac{Nb^2}{3} \right)^{\frac{1}{2}}.
$$

Show that the *relative* fluctuation of the contour length decreases with increasing chain length, i.e. that the fixed contour length assumption is justified for extremely long chains.

4-3. Can you guess what the effect of contour length fluctuations will be on the disentanglement times of entangled, but not extremely long, polymer chains? [Hint: See the first equality in Eq. (4.19)]. What will be the consequence for the viscosity of such polymer chains compared to the tube model prediction?

Index